J Musculoskelet Neuronal Interact 2010; 10(3):220-230

Original Article

Hylonome

A thermodynamic model of bone remodelling: the influence of dynamic loading together with biochemical control

V. Klika[1,2], F. Maršík[1]

[1]Institute of Thermomechanics, v.v.i., Academy of Sciences of Czech Republic, Dolejškova 5, 182 00 Prague, Czech Republic;
[2]Dept. of Mathematics, FNSPE, Czech Technical Univerzity in Prague, Trojanova 13, Prague, Czech Republic

Abstract

Understanding of the bone remodelling process has considerably increased during the last 20 years. Since the ability to simulate (and predict) the effects of bone remodelling offers substantial insights, several models have been proposed to describe this phenomenon. The strength of the presented model is that it includes biochemical control factors (e.g., the necessity of cell-to-cell contact, which is mediated by the RANKL-RANK-OPG chain during osteoclastogenesis) and mechanical stimulation, the governing equations are derived from interaction kinetics (e.g., mass is preserved in running reactions), and the parameters are measurable. Behaviour of the model is in accordance with experimental and clinical observations, such as the role of dynamic loading, the inhibitory effect of dynamic loading on osteoclastogenesis, the observation that polykaryon osteoclasts are activated and formed by a direct cell-to-cell contact, and the correct concentrations of osteoblasts, osteoclasts, and osteocytes. The model does not yet describe the bone remodelling process in complete detail, but the implemented simplifications describe the key features and further details of control mechanisms may be added.

Keywords: Bone Remodelling, Chemical Kinetics, RANKL-RANK-OPG Chain, Dynamic Loading

Introduction

A great advance in understanding mechanosensing and mechanotransduction of bone tissue has occurred in the past years. However, a clear answer is yet to come. There is plentiful evidence that most cells in human body are able to sense their mechanical environment, including osteoblasts and osteocytes. Li et al. found that marrow stromal cells change their proliferation rate and gene expression patterns in response to mechanical stimulation[1]. Ehrlich and Lanyon mention that osteocytes produce significantly higher levels of PGE_2 (prostaglandin E_2) and PGI_2 (prostacylin) than osteoblasts and *in vivo* inhibition of prostaglandins prevents bone adaptation in response to mechanical strains[2]. Further, nitric oxide NO is also a mediator of mechanically induced bone formation. It is released, similarly, as prostanoids, in higher levels after exposure to physiological levels of mechanical loading. Moreover, Rubin discovered that dynamic loading down-regulates osteoclastic formation[3] (more precisely, the strained bone cell downregulates its expression of RANKL[4]), which suggests that mechanical forces play an important role in bone adaptation process.

Candidate mechanoreceptors within a cell are stretch-activated channels, integrins (membrane spanning proteins that couple the cell to its extracellular environment), connexins (membrane spanning proteins that form channels that allow the direct exchange of small molecules with adjacent cells - including intercellular communication via gap junctions), and membrane structure[5]. Nowadays, there is also a completely different possible explanation for transformation mechanical signal into a biochemical function. Valle et al. explain in their review that only a proper mechanical loading may lead to exposure of binding sites and thus enabling further biochemical processes to proceed[6]. Most probably multiple mechanosensors are involved in receiving mechanical signals. Moreover, there are other studies showing the importance of many other mechanisms beside those mentioned above[7,8].

On tissue level, it is clear that mechanical loading is important in the bone remodelling process. Heřt described an interaction between the mechanical stimulation of local cells and

The authors have no conflict of interest.

Corresponding author: Dr. Václav Klika, Trojanova 13, Prague 2, 12000, Czech Republic
E-mail: klika@it.cas.cz

Edited by: F. Rauch
Accepted 30 March 2010

the bone adaptation process in the 1970s[9], Frost observed the same behaviour in his clinical praxis and summed it up in his "Utah paradigm"[10,11]. More recently, the fundamental importance of dynamic loading was accepted. Comparison of the static versus the dynamic loading effects on bone remodelling is given in a nice and inspectional review by Ehrlich and Lanyon[2]. Further, Robling provides experimental results that confirm the essential importance of the dynamic loading[12]. It is worth mentioning that Heřt referred to this fact in his observations more than 35 years ago[9].

In the presented manuscript, the mechanical stimulation of bone remodelling was simply assumed to be proportional to rate of volume change (for details see reference 13). As it will be seen from the features and results of the model, it seems to capture the response of bone to changes of its mechanical environment on tissue level. Probably, the other ways of mechanosensing are controlling the triggering of bone remodelling process in a given loci. We realize that biochemical reactions are initiated and influenced primarily by genetic effects and then by external biomechanical effects (stress changes). The aim of the presented thermodynamic model is to combine biological and biomechanical factors whereas currently available models of bone remodelling focus only on one of these factors which is actually the reason why this model was developed. It should provide an estimate of the effects of increased physical activity on quality of bone even in several disease states. Such a model may also reflect changes in remodelling behaviour resulting from pathological changes to the bone metabolism or from hip joint replacement and also may help for better assessment of the risk of osteoporosis-related fractures[14]. Preliminary version of the mentioned approach has been published by our team in the past[15,16] but not until this considerably improved version was the model applicable to praxis (both qualitative and quantitative results).

Methods

Bone remodelling is a very complex mechanism. It is necessary to make reasonable simplification to identify the essential control mechanisms. The presented model covers the accepted crucial features[17].

In this manuscript, several schemes for treating cellular interactions (as interactions among mixtures of chemical substances) are proposed, which are commonly used in similar problems[18,19]. In our model, individual components of bone are substrates and products of biochemical interactions, whose rates are determined by the difference in chemical potentials. The affinity and chemical potential are (in simpler cases) proportional to the logarithm of the molar concentration of the involved substances[20] as shown equation (6). This is actually a modified version of the law of mass action with the additional effect of dynamic loading on the interaction rates[13]. The law of mass action is frequently used in modelling biological processes[19]. However, it is only a simplified model that can be justified by agreement between calculated data and clinical observations. From the submitted results, it can be seen that features of the presented model are consistent with clinical and experimental data.

Finding a reasonable description of bone remodelling

The only cells that resorb bone tissue are osteoclasts. They are activated by fusing into a multinucleated complex. This interaction forms a new substance, MNOC, by fusion of *MCELL* in the presence of the essential cell-to-cell interaction, *RR*. This can be described by the following Menten-Michaelis-like mechanism, which is supported by the observation that RANKL activates osteoclasts in a dose-dependent manner[21],

$$RR + MCELL \overset{k_{\pm 1}}{\longleftrightarrow} MNOC + N_4 \quad \textbf{(1)}$$

In this scheme *RR* describes the ligand-receptor bonds (RANKL-RANK) between *OB* and *MCELL* (precursor of osteoclast) that enable formation of the multinucleated osteoclasts, MNOC, from mononuclear cells (*MCELL*). N_4 is a remaining product of reaction (1). The RANKL-RANK-OPG chain is delegated in the presented model by the term *RR* - RANKL-RANK, which is the outcome of the control mechanism. However, the whole chain can be added through this term because binding among the ligand, receptor, and decoy receptor are much faster than the considered processes of bone remodelling and thus, the RANKL-RANK-OPG kinetics may be treated independently58. This presented model only treats the necessary cell-to-cell interaction (mediated by RANKL-RANK-OPG chain) for osteoclastogenesis.

It is assumed that bone decomposition can be characterised by the following reaction scheme,

$$MNOC + Old\_B \overset{k_{\pm 2}}{\longleftrightarrow} N_6 + LF \quad \textbf{(2)}$$

where Old_B denotes old bone. During resorption, the osteoclasts release local factors, *LF*, (mainly growth factors) from bone, which play a role in the activation of osteoblasts[22]. This assumption is a simplification of a cascade of reactions, but it is supported by the observations that are presented in the Results section. Moreover, it is supported by the observation that the old bone concentration, which is actually the molar concentration of osteocytes present in the old bone tissue (see parameters setting for more detailed explanation), is a dose-dependent function of the molar concentrations of the bone resorbing agents, MNOC. Similarly, the molar concentration of osteoclasts decreases as bone is resorbed because the local factors such as *TGF-β* are released during resorption. Because *TGF-β* promotes osteoclast apoptosis[23,24], it was observed that bone resorption causes a decrease in MNOC.

Local factors released from the bone matrix activate *osteoprogenitor* cells that proliferate and differentiate into osteoblasts *OB*, which secrete *osteoid* (nonmineralised bone - organic part of bone tissue)[22]. Thus, the behaviour of osteoblasts at a specific site can be represented by reaction schemes

$$LF + osteoprogenitor \overset{k_{\pm 3}}{\longleftrightarrow} OB + N_{10} \quad \textbf{(3)}$$

and

$$OB + N_{11} \overset{k_{\pm 4}}{\longleftrightarrow} Osteoid + N_{13} \quad \textbf{(4)}$$

where N_{10}, N_{13} are remaining substrata. The first scheme (3) represents *OB* formation of osteoblasts from osteoprogenitor cells under the control of local factors. Secretion of osteoid may be described by scheme (4), because osteoblasts, *OB*, supported with the needed substances, N_{11}, secrete osteoid and may become embedded in the newly formed bone tissue. This supports the idea that osteoblast concentration decreases as osteoid is formed, as described by (4).

The longest timescale in the bone remodelling process pertains to mineralisation of the osteoid, which involves deposition of calcium and other minerals, N_{14}, into matrix. The ossification of *osteoid* (the primary ossification) into new bone tissue after addition of appropriate substances, N_{14}, may be characterised by the following scheme,

$$N_{14} + Osteoid \xleftrightarrow{k_{\pm 5}} New\_B + N_{16} \qquad \textbf{(5)}$$

where New_B denotes a new bone formed by the remodelling process and N_{16} is the residuum of the bone formation reaction.

Model formulation

Klika and Maršík showed that there is a coupling effect between mechanical loading and chemical interactions and that it was necessary to treat dynamic loading as a stimulatory mechanism. Moreover, they shown that chemical and mechanical processes both facilitate one another and may play a triggering role for the other coupled processes.

The interaction schemes (1)-(5) describe the essential processes of bone remodelling. There are 16 substances involved, which are noted as N_i, and their concentrations as $[N_i]$; $\nu'_{\alpha i}$ and are the stoichiometric coefficients of the mixture of substances N_i entering and resulting from reaction α, respectively. To obtain the time evolution of the molar concentrations of these substances, the modified law of mass action (which reduces to the standard form when $r_\alpha = l_{\alpha\alpha} A_\alpha$) was used[13] with the addition of inflow and outflow fluxes, J_i,

$$[\dot{N}_i] = \sum_{\alpha=1}^{5} (\nu'_\alpha - \nu_{\alpha i})\, r_\alpha + J_i \qquad \textbf{(6)}$$

$$r_\alpha = l_{\alpha\alpha} A_\alpha + l_{\alpha v} d_{(l)} = k_{+\alpha} \prod_{i=1}^{n} [N_i]^{\nu'_{\alpha i}} - k_{-\alpha} \prod_{i=1}^{n} [N_i]^{\nu_{\alpha i}} - l_{\alpha v} d_{(l)} \qquad \textbf{(7)}$$

where $k_{+\alpha}$ and $k_{-\alpha}$ are the forward and backward reaction rate constants.

A system of 16 ODEs was obtained. If fluxes are assumed to be constant in time, the existence of stationary solution describes the following relations among the substance concentrations,

$$\begin{aligned}
&[RR] = B_1 + [MCELL] \qquad \textbf{(8)}\\
&[MNOC] = B_3 - [MCELL] + [Old_B]\\
&[N_4] = B_4 - [MCELL]\\
&[N_6] = B_6 - [Old_B] - ([New_B] + [Osteoid] + [OB])\\
&[LF] = B_7 - [Old_B]\\
&[osteoprogenitor] = B_8 - ([New_B] + [Osteoid] + [OB])\\
&[N_{10}] = B_{10} + ([New_B] + [Osteoid] + [OB])\\
&[N_{11}] = B_{11} - ([New_B] + [Osteoid])\\
&[N_{13}] = B_{13} + ([New_B] + [Osteoid])\\
&[N_{14}] = B_{14} - [New_B]\\
&[N_{16}] = B_{16} + [New_B]
\end{aligned}$$

where $B_i = \beta_i$ [Bo] and [Bo] and β_i are defined in section 3. These eleven relations enable to decrease the number of independent variables in the system of sixteen ODEs. Further, it was assumed that the forward reaction is dominant in all considered reactions, which means $k_{+\alpha} >> k_{-\alpha}$. The last step is normalisation by the factor $1/(k_{+2}[Bo]^2)$. Finally, we obtain the following system of dimensionless differential equations for five independent variables,

$$\frac{dn_{MCELL}}{d\tau} = -\delta_1 (\beta_1 + n_{MCELL}) n_{MCELL} + J_3 + J_{New\_B} - D_1 \qquad \textbf{(9)}$$

$$\frac{dn_{Old\_B}}{d\tau} = -(\beta_3 - n_{MCELL} + n_{Old\_B}) n_{Old\_B} - D_2 + J_{New\_B} \qquad \textbf{(10)}$$

$$\begin{aligned}
\frac{dn_{OB}}{d\tau} = {} & \delta_3 (\beta_6 - n_{Old_B} - (n_{OB} + n_{Osteoid} + n_{New_B})) \cdot \\
& \cdot (\beta_8 - (n_{OB} + n_{Osteoid} + n_{New_B})) - \\
& - \delta_4 (\beta_{11} - (n_{Osteoid} + n_{New_B}) n_{OB}) + D_3 - D_4
\end{aligned} \qquad \textbf{(11)}$$

$$\begin{aligned}
\frac{dn_{Osteoid}}{d\tau} = {} & \delta_4 (\beta_{11} - (n_{Osteoid} + n_{New_B})) n_{OB} - \\
& - \delta_5 (\beta_{14} - n_{New_B}) n_{Osteoid} + D_4 - D_5
\end{aligned} \qquad \textbf{(12)}$$

$$\frac{dn_{New\_B}}{d\tau} = \delta_5 (\beta_{14} - n_{New\_B}) n_{Osteoid} - J_{New\_B} + D_5 \qquad \textbf{(13)}$$

where index i specifies the substances, index α specifies the reactions, β_i is the sum of normalised initial molar concentrations of relevant substances, δ_α relates to the interaction rate, D_α describes the influence of dynamic loading on reactions, n_i is the normalised concentration of the i-th substance, and J_3 is a normalised outflow of MNOC (i.e., MNOC apoptosis) and J_{New_B} is the normalised outflow of new bone New_B into old bone Old_B (see equation (22) on this matter). Parameter values estimation as well as their interpretation is the topic of the following section.

By solving these kinetic equations, the time evolution of *MCELL,* Old_B*, OB, Osteoid*, and New_B concentrations can be obtained.

Parameters setting

All of the parameters in this model are physically reasonable and measurable. Unfortunately, we do not yet have enough experimental constraints for of all of them. However, we can provide reasonable estimates based on experiments and current knowledge of the process. The first step was to determine the parameters δ_α. Since ODEs (9)-(13) are in dimensionless form, the parameters representing the interaction rates can be assigned from the ratios of these rates,

$$\delta_\alpha = \frac{k_{+\alpha}}{k_{+2}} \qquad \textbf{[1]}$$

where k_{+2} represent the interaction rate of the second reaction scheme.

In the literature, it was noted that differentiation of MNOC (reaction scheme (1)) lasted 4-7 days[25] so 5 days was chosen

for this parameter. Resorption carried out by MNOC (the second reaction scheme (2)) was found to last 20 days[12]. Further, the reversal phase (the third reaction scheme (3)) was found to take 9-10 days[12,22]. Osteoid production by *OB*, which is the slowest process in bone remodelling, was found to last 90-140 days[12,22]. Consecutive mineralisation is nearly an indefinite process, but primary ossification, which completes the formation of new bone from osteoid, has a timescale similar to osteoid formation[26]. In summary, the parameters δ_α are

$$\delta_1 = \frac{k_{+1}}{k_{+2}} = \frac{T_2}{T_1} \cong \frac{20\text{days}}{5\text{days}} = 4$$

$$\delta_3 = \frac{k_{+3}}{k_{+2}} = \frac{T_2}{T_3} = \frac{20\text{days}}{9\text{-}10\text{days}} \cong 2$$

$$\delta_4 = \frac{k_{+4}}{k_{+2}} = \frac{T_2}{T_4} = \frac{20\text{days}}{140\text{days}} = \frac{1}{7} \cong \delta_5$$

To further constrain the parameters, estimates of the resorption rate of bone (Old_B) are required. Kanehisa[27] found that a single MNOC resorbs 43 μm^3 to 1225 μm^3 of bone per hour with a mean value of 390 $\mu m^3/hr$, which was the value used. To obtain the total resorption rate in bone, an estimation of the total active MNOC in the body was needed. In a typical BMU (basic multicellular unit[28,29]) there are nine MNOC "at the front" of the cutting cone and approximately 2000 *OB*s at the end[30]. These quantities for MNOC, in BMU, may be verified by Eriksen's observation that the typical osteoclast (MNOC) diameter is 50 μm[31]. Thus, 9 or 10 MNOCs fill the front line of the "cutting cone"[29] with diameters of 200-250 μm. Further, Manolagas states that 1 million BMU operate at any moment in the body[32]. If we use these data, the resorption in the human body per hour is

$$390 \cdot 9 \cdot 10^6\ \mu m^3/h \cong 3.5\ mm^3/\text{h} \qquad \textbf{(14)}$$

In other words, the entire skeleton, which has a volume of 33, would be resorbed in $1.75\ 10^6/3.5 = 5\ 10^5 h \cong 57$ years. In contrast, it is often stated that the skeleton remodels once every 5-7 years. From this observation it is apparent that the assertion of Manolagas should be modified to state that approximately 10^7 BMU operate at any moment in the body rather than 10^6.

Now it is possible to determine the molar concentration of MNOC, *OB*, and Old_B in human bone as

$$[\text{MNOC}] = \frac{9\ 10^7}{N_A} = \frac{1}{1.75}\frac{mol}{l} \cong 5.14\frac{10^7}{N_A}\frac{mol}{l} \qquad \textbf{(15)}$$

$$= \frac{2000\ 10^7}{N_A}\frac{1}{1.75}\frac{mol}{l} \cong 1.1\frac{10^{10}}{N_A}\frac{mol}{l} \qquad \textbf{(16)}$$

where N_A represents Avogadro's number. The fact that ODEs (9)-(13) describe the bone remodelling process in dimensionless form is useful for mathematical analysis. One consequence is that all of the concentrations are normalised relative to the concentration of bone tissue - osteocytes. It is often stated that MNOC and *OB* comprise around of cells in human bone. Robling has stated that the ratio of [OCy] to ([OB]+[MNOC]) is around 20[12], which also supports our assertion that [OCy] is a determining factor for bone tissue concentration, and this information yields a useful constraint (20 ([OB]+[MNOC]) = [OCy]). In this model [Old_B] = [OCy]. This definition is equivalent to the assumption that the density of bone tissue ρ is proportional to the number of *OCy* in given volume, or that the molar concentration of *OCy* is constant in tissue; the amount of bone tissue in a given volume determines the local bone density.

A correct estimation of reaction rate, k_{+2}, is crucial for finding a relation between the real time, t, and the dimensionless reduced time, $\tau = t\ k_{+2}[\text{Bo}]$, where [Bo] is the initial concentration of bone tissue ([Bo] = [Old_B_0]+[New_B_0]). From the second reaction (2),

$$\frac{[\text{Old\_B}]}{[\text{Old\_B}_0]} = \exp\left(-k_{+2}[\text{MNOC}]\,\Delta t\right) \qquad \textbf{(17)}$$

where [Old_B_0] and [Old_B] are the concentrations of bone at $t=\Delta t$ and $t=t$, respectively. To set k_{+2}, the concentration change of old bone caused by MNOC needs to be calculated. It was determined that a single MNOC dissolves an average of 390 $\mu m^3/h$ of bone tissue. Since

$$[\text{Old\_B}] = [\text{OCy}] \cong 20[\text{OB}]$$

we have

$$[\text{Old\_B}] = 22\ \frac{10^{10}}{N_A}\ \frac{mol}{l} = 2.210^{-4}\ \frac{1}{N_A}\ \frac{mol}{\mu m^3} \qquad \textbf{(18)}$$

which implies that there is approximately one *OCy* per 5000 μm^3. To verify this number, as well as the previous estimates, the average distance between *OCy* can be calculated by $\text{dist} = \sqrt[3]{5000} - \sqrt[3]{3}\sqrt[3]{5000} \cong 17 - 29\ \mu m$,

which is consistent with Sugawara's observation of 24.1±2.8 μm[34]. In summary, one MNOC dissolves $3.9\ 10^2 \cdot 2\ 10^{-4} = 7.8\ 10^{-2}$ of *OCy* per hour, or $\frac{7.8\ 10^{-2}}{3.6\ 10^3} = 2.17\ 10^{-5}\ OCy$ per second. Without loss of generality, it can further be assumed that this rate is independent of the MNOC concentration because it is noncompeting. Finally, the rate of change of [Old_B] is given by (using equation (15)),

$$\frac{\Delta[\text{Old\_B}]}{\Delta t = 1s} = \frac{\Delta[\text{OCy}]}{1s} = \frac{5.14\ 10^7 \cdot 2.17\ 10^{-5}}{N_A} \cong \frac{1.12\ 10^3}{N_A}\ \frac{mol}{ls}$$

and thus, the value of k_{+2} should satisfy the expression (using relation (17)),

$$\frac{[\text{Old\_B}]}{[\text{Old\_B}_0]} = \frac{[\text{Old\_B}_0] - \Delta[\text{Old\_B}]}{[\text{Old\_B}_0]} =$$

$$= \frac{22\ 10^{10} - 1.12\ 10^3}{22\ 10^{10}}\ \frac{N_A}{N_A} = 1 - \frac{5.1}{10^9} =$$

$$= \exp\left(-k_{+2} \cdot \frac{5.14\ 10^7}{N_A}\right) = \sum_{n=0}^{\infty} \frac{\left(-k_{+2} \cdot \frac{5.14\ 10^7}{N_A}\right)^n}{n!} \approx$$

$$\approx 1 - k_{+2} \cdot \frac{5.14\ 10^7}{N_A} \cdot$$

By solving the last equation, one obtains

$$k_{+2} = \frac{5.1}{5.14}\ \frac{N_A}{10^{16}} \cong 6.0\ 10^7 \frac{l}{mol \cdot s} \cdot \qquad \textbf{(19)}$$

Interestingly, this value also could have been inferred by assuming that *OCy* were located so that they are 'tuned' together to

communicate. The speed of sound propagation in bone is around 2900 m/s[35] and the typical distance between *OCy* is 20 μm, which corresponds to $\lambda/2$, and yields

$$f = \frac{2900\ m/s}{2 \cdot 20\ 10^{-6}\ m} \Rightarrow T = \frac{2\pi}{f} = \frac{8\pi}{29} 10^{-7}\ s$$

Since the concentration changes in time are proportional to the concentration with the rate coefficient $k_{+\alpha}$, it holds that

$$\frac{\mathrm{d}c}{\mathrm{d}t} = -k_{+\alpha}c \Rightarrow \frac{c(t)}{c_0} = \exp(-k_{+\alpha}t) \qquad \textbf{(20)}$$

It is noted that $\frac{1}{k_{+\alpha}}$ is the characteristic time and, from (20), that $k_{+\alpha} \sim \frac{1}{T} \cong \frac{29}{8\pi} 10^7 \cong 1.15\ 10^7$, which is consistent with the previous estimate. It would be interesting to test the second hypothesis by observing if the distance between *OCy* is crucial for proper mechanosensing and bone adaptation.

Knowledge of k_{+2} allows for the relation between the computational time, τ, and real time, t, to be determined as,

$$\tau = k_{+2}[\mathrm{Bo}]t = 6.0\ 10^7 \cdot \frac{22\ 10^{10}}{\mathrm{N_A}} t \cong 2.2\ 10^{-5}\ t$$

It is useful to note values of τ that are equivalent to 1 day and to the duration of the bone remodelling cycle ($5d$+$20d$+$9d$+$140d$+$140d \approx 315d$)

$$\tau_{day} = 2.2\ 10^{-5} \cdot 24 \cdot (60)^2 \cong 1.9 \qquad \textbf{(21)}$$
$$\tau_{BR} = \tau_{day} \cdot 315 = 598.5$$

Bone remodelling creates a new bone after 315 days by replacing old bone tissue. This new bone tissue, as it is called, is merely regular bone tissue that has been recently formed, and has reduced mineral content since the secondary ossification has not yet begun. Nevertheless, it can be remodelled if needed. This model has the same features; it creates new bone tissue that is transformed into Old_B. This transformation is realized by fluxes of particular substances, namely the outflow of *New_B* (J_{New_B}) and the inflow of *Old_B* (J_{Old_B}). In this model,

$$\mathrm{J}_{Old\_B} = \mathrm{J}_{New\_B} \qquad \textbf{(22)}$$

which guarantees that one mol of New_B is changed into one mol of Old_B. Henceforth, Old_B may simply be referred to as *Bone* and New_B as *formation index* because the formed new bone New_B transforms into old bone, which represents total amount of bone. This allows for J_{Old_B} to be calculated. It was concluded that one MNOC resorbs 390 $\mu m^3/h$ and in the entire skeleton there are $9\ 10^7$ MNOCs, which implies that 3.510^{10} $\mu m^3/h = 35\ mm^3/h$ of bone tissue is removed. Because bone tissue is mostly in equilibrium (resorption is balanced with formation), it may be assumed that equivalent amounts of bone are produced and resorbed,

$$\frac{\mathrm{d}}{\mathrm{dt}}[\mathrm{Old\_B}] = \text{resorbtion terms} - \mathrm{J}_{\mathrm{Old\_B}}^{equilib} = 0$$

$$\Downarrow$$

$$\mathrm{J}_{\mathrm{Old\_B}} = \text{resorbtion terms} = 35\ mm^3/h \cong 10^7\ \mu m^3/s,$$

and thus, the amount of bone resorbed per second is

$$\frac{\Delta \#Old\_B}{\Delta t} = 10^7 \cdot 2.2\ 10^{-4}/\mathrm{N_A} = 2.2\ 10^3/\mathrm{N_A}\ mol \cdot s^{-1}$$

where equation (18) was used. When considering that the skeleton has a typical volume of $1.75l$, it may be concluded that

$$\frac{\Delta[\mathrm{Old\_B}]}{\Delta t} = \frac{2.2\ 10^3}{1.75/\mathrm{N_A}} = \frac{1.25\ 10^3}{\mathrm{N_A}} \frac{mol}{l \cdot s} = \mathrm{J}_{\mathrm{Old\_B}} \qquad \textbf{(23)}$$

$$\Rightarrow \mathrm{J}_{\mathrm{Old\_B}} = \mathrm{J}_{\mathrm{Old\_B}} \cdot \frac{1}{k_{+2}[\mathrm{Bo}]^2} \cong 2.6\ 10^{-4} \qquad \textbf{(24)}$$

Bone remodelling is a long process. Participating cells must be replaced several times. This fact is exploited by the body itself as a control mechanism, for example when estrogen promotes osteoclast apoptosis[30]. The apoptosis of MNOC plays a substantial role since its mean life *in vivo* is 3 days[36]. Using this knowledge, we may determine J_3 (=negative flux of MNOC=MNOC apoptosis) similarly to (23) as

$$\text{decrease of [MNOC]}/s = \frac{\#MNOC}{volume \cdot time} = \frac{9\ 10^7}{1.75l \cdot 3 \cdot 24h} = \frac{2.0\ 10^2}{\mathrm{N_A}} \frac{mol}{l \cdot s}$$

$$\Rightarrow \frac{\mathrm{J}_3}{\mathrm{J}_{\mathrm{New\_B}}} = \frac{2\ 10^2}{\mathrm{N_A}} \cdot \frac{\mathrm{N_A}}{1.25\ 10^3} = \frac{4}{25}$$

Another family of parameters, β_i, can be determined by the following sum of normalised initial concentrations,

$$\beta_6 = \frac{[\mathrm{Old\_B_0}] + [\mathrm{New\_B_0}] + [\mathrm{Osteoid_0}] + [\mathrm{OB_0}]}{\mathrm{Bo} = [\mathrm{Old\_B_0}] + [\mathrm{New\_B_0}]} + \frac{[\mathrm{N_{60}}]}{[\mathrm{Bo}]} \cong$$

$$\cong 1 + \frac{[\mathrm{Osteoid_0}] + [\mathrm{OB_0}] + [\mathrm{N_{60}}]}{[\mathrm{Old\_B_0}]} = 1 + \frac{0 + 1/20[\mathrm{Old\_B_0}] + 0}{[\mathrm{Old\_B_0}]} = 1.05$$

where the relation between *OB* and *OCy* was used, and it was assumed that the remaining product (N_6) and osteoid are not present in the volume where bone remodelling initiates. Similarly,

$$\beta_3 = \frac{[\mathrm{MNOC_0}] - [\mathrm{Old\_B_0}] + [\mathrm{MCELL_0}]}{[\mathrm{Bo}]} = \frac{1}{2000} \qquad \textbf{(25)}$$

$$\beta_1 = \frac{[\mathrm{RR_0}] - [\mathrm{MCELL_0}]}{[\mathrm{Bo}]} = 0.6 \qquad \textbf{(26)}$$

$$\beta_{11} = \frac{[\mathrm{New\_B_0}] + [\mathrm{Osteoid_0}] + [\mathrm{N_{110}}]}{[\mathrm{Bo}]} = 1 \qquad \textbf{(27)}$$

$$\beta_{14} = \frac{[\mathrm{New\_B_0}] + [\mathrm{N_{140}}]}{[\mathrm{Bo}]} = \frac{1}{20} \qquad \textbf{(28)}$$

$$\beta_8 = \frac{[\mathrm{osteoprogenitor_0}] + [\mathrm{New\_B_0}]}{[\mathrm{Bo}]} + \frac{[\mathrm{Osteoid_0}] + [\mathrm{OB_0}]}{[\mathrm{Bo}]} = \frac{1}{10} \qquad \textbf{(29)}$$

The last group of parameters, D_α, describes the effect of dynamic loading on the rate of reactions as

$$\mathrm{D}_\alpha = \frac{l_{\alpha v} d_{(l)}}{k_{+2}[\mathrm{Bo}]^2}\ [1] \qquad \textbf{(30)}$$

where equation (30) follows from the law of mass action (6), the linear relation $r_\alpha = l_{\alpha v} d_{(l)} + l_{\alpha\alpha} \mathsf{A}_\alpha$ (see [13]) between reaction rate and mechanical loading was used and the denominator is the factor that transformed the ODEs into dimensionless form (9)-(13).

As equation (30) shows, the influence of mechanical loading on each reaction scheme, $l_{\alpha v}$, must be determined. The unknown parameters $l_{\alpha v}$ were calculated from the solution to the constraint extremum problem such that the effects of mechanical loading

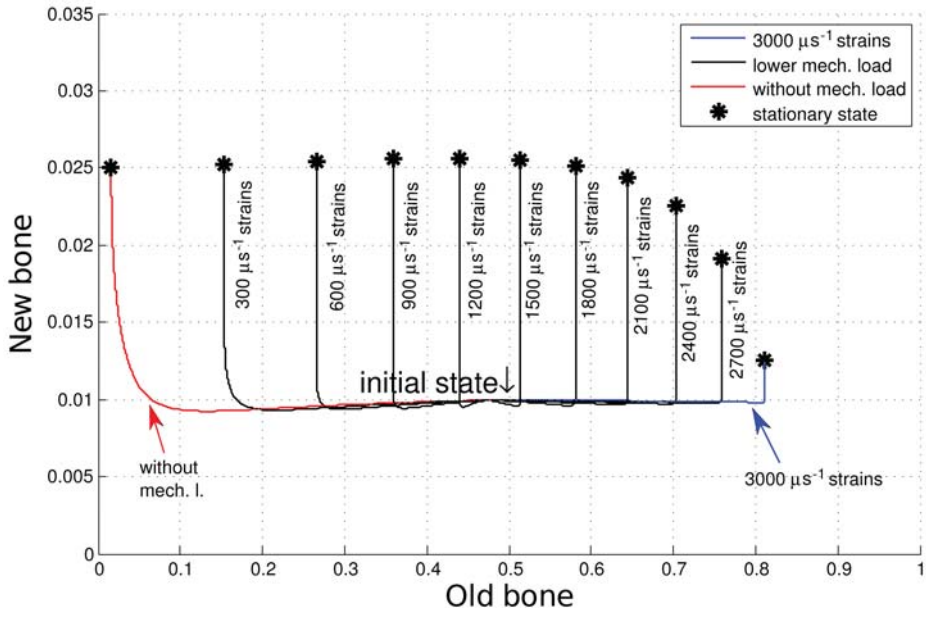

Figure 1. The evolution of the old bone and new bone concentrations in phase space under various loading conditions. The positivity of [Old_B] and [New_B] can be seen. Furthermore, as the stimuli rises (higher loading case), the bone density (proportional to the sum of [Old_B] and [New_B]) in the stationary state increases proportionally.

matched the observations, namely $\rho \in (0.1\ g\ cm^{-3}, 2.0\ g\ cm^{-3})$[37]. This implies that $\rho_{max}/\rho_{min} = \rho_{cort,max}/\rho_{spongy,min} = 20$. This assumption is supported by the work of the Hedgecock[38], who noticed that the number of apoptotic osteocytes in bone was linearly proportional to the number of osteons in a given volume of human bone. Since the ratio of apoptotic osteocytes is approximately constant at 10% of osteocytes[38], we may conclude that osteon density is linearly proportional to osteocyte density. Moreover, the positivity of the stationary solution (and the terms in the square roots of equations (B.1)) is guaranteed by satisfying constraints on the parameters. However, the condition guaranteeing the positivity of $\overline{n_{New\_B}}$ is rather complex and is treated separately. The last two constraints ensure the correct number of cells in the model results (see above), namely [MNOC]/[OB] = 1/220 and [OB] = 4.5% of bone cells. Since the results are in normalised concentrations, all molar concentrations of bone cells, *OCy, OB,* MNOC, will have the correct values.

To summarise, D_α are calculated from the following extremum problem:

$$\min_{D_\alpha} |[OB]\% - 4.5\%| \qquad \textbf{(31)}$$

with constraints:

$$\frac{\rho_{max}}{\rho_{min}} = 20 \qquad \textbf{(32)}$$

$$[MNOC]\% = 0.023\% \Leftrightarrow \frac{OB}{[MNOC]} = \frac{2000}{9} \cong 220 \qquad \textbf{(33)}$$

and under the condition that all concentrations are positive. It is known that spongy bone experiences smaller deformations/strains and cortical bone provides weight-bearing support on the outer cortex. These facts were used to set $l_{\alpha v}$ such that the maximal density(found in cortical bone - the properly loaded case) and the minimal apparent density (found in spongy bone - the unloaded case) in the stationary state satisfied the relations

$$\rho = \rho(d_{(1)}) \Rightarrow \frac{\rho_{max}}{\rho_{min}} = \frac{\rho_{cort,\,max}}{\rho_{spongy,\,min}} = \frac{2.0\ g/cm^3}{0.1\ g/cm^3} = 20$$

which yield the correct range for apparent bone density[37,39]. Equation (31) ensures that the percentage of osteoblasts *OB* in the stationary state will be and relation (33) ensures the correct MNOC percentage.

In addition to the fact that the stationary concentrations are positive, the parameters $l_{\alpha v}$ that solve the aforementioned extremum problem also guarantee that the concentrations remain positive for all time, $t>0$, and are listed in appendix A.

Results

As discussed in section 3, all of the concentrations of substances N_i are positive for all time $t>0$. This crucial condition needs to be satisfied for every model that is based on a biochemical description.

The differential equations (9)-(13) have been solved numerically. To illustrate the predicted response of bone remodelling to various stimuli, the results for several loading cases were calculated and were plotted in phase space, which appear in Figure 1. It can be seen that the stationary state bone density (proportional to sum of Old_B and New_B) increases with increasing stimuli (higher loading case). More precisely, this ratio is 20 as the input criteria dictate (32). The case with the

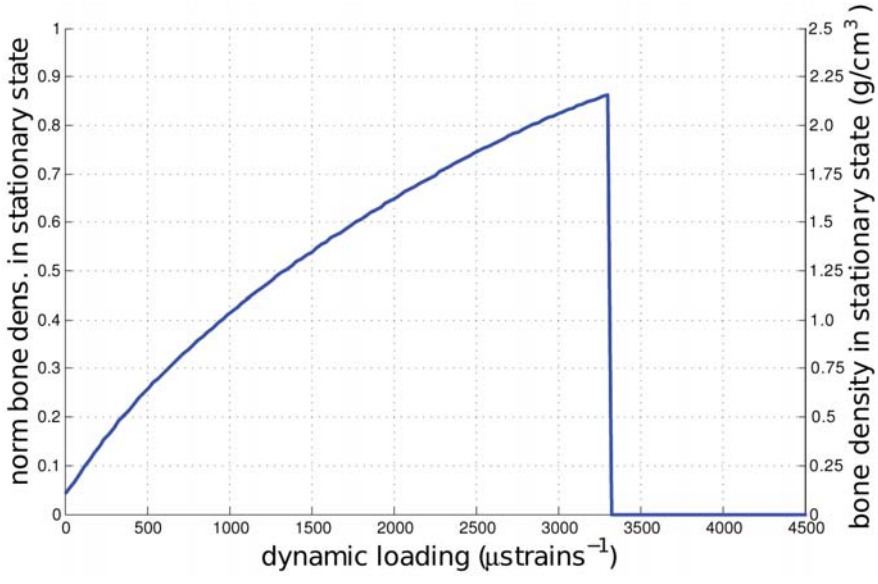

Figure 2. The Frost diagram predicted using this model. The values of normalised bone density as a function of dynamic loading in the stationary state are plotted. Axis on right-hand-side shows probable bone density values (bone density is assumed to be proportional to the osteocyte concentration, OCy, in bone).

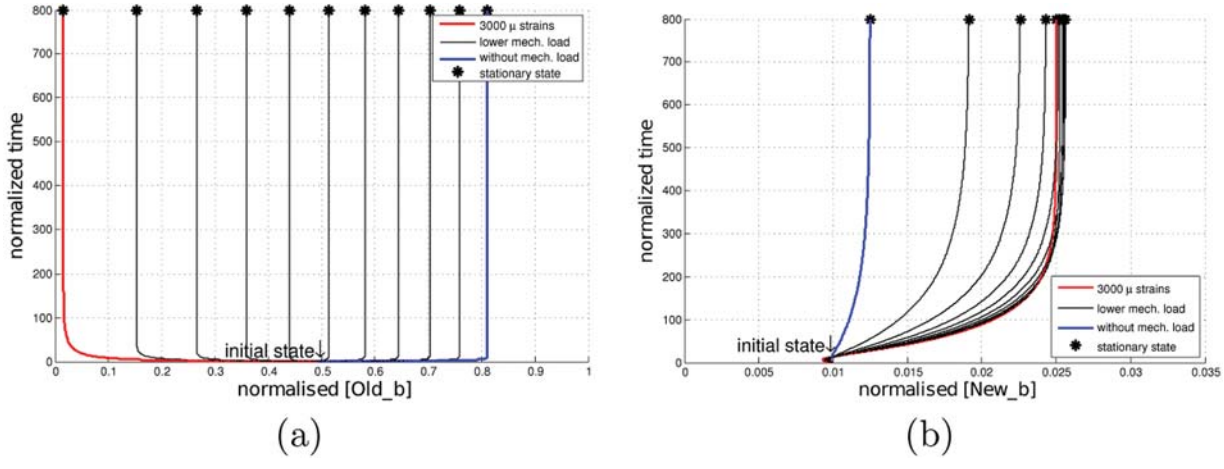

Figure 3. (a) The predicted time evolution of [Old_B], which shows that resorption of old bone should stop after τ≅30-40, which is equal to 17-23 days and is consistent with the literature. (b) Time evolution of [New_B]. Similarly, it can be seen that the predicted time of new bone formation is approx. 300-400 days.

highest bone density resulted from the greatest stimuli found in bone, 3000 $\mu\varepsilon$[12]. The bone density decreases with decreasing mechanical stimulus. In the absence of stimuli, biochemical factors prevail and the bone density does not drop to zero.

It is useful to consider the normalised density values in the stationary state as a function of dynamic loading, which appears in Figure 2. This provides a more condensed view of the bone response to mechanical stimulation. Moreover, if the time evolution is considered (Figure 3), it is noted that Old_B reaches its stationary state in $\tau_{\text{Old\_B}}$≅30–50 and New_B in $\tau_{\text{New\_B}}$≅450–600. From (21), $T_{\text{Old\_B}}$≅16–26 days and $T_{\text{New\_B}}$≅ 237–316 days, which is in a very good agreement with current knowledge about the duration of particular phases of bone remodelling (see section 3).

So far, only the influence of mechanical stimuli on bone remodelling was investigated. One great advantage of the presented model is that it allows for the influence of dynamic load and biochemical changes to be investigated; one may observe

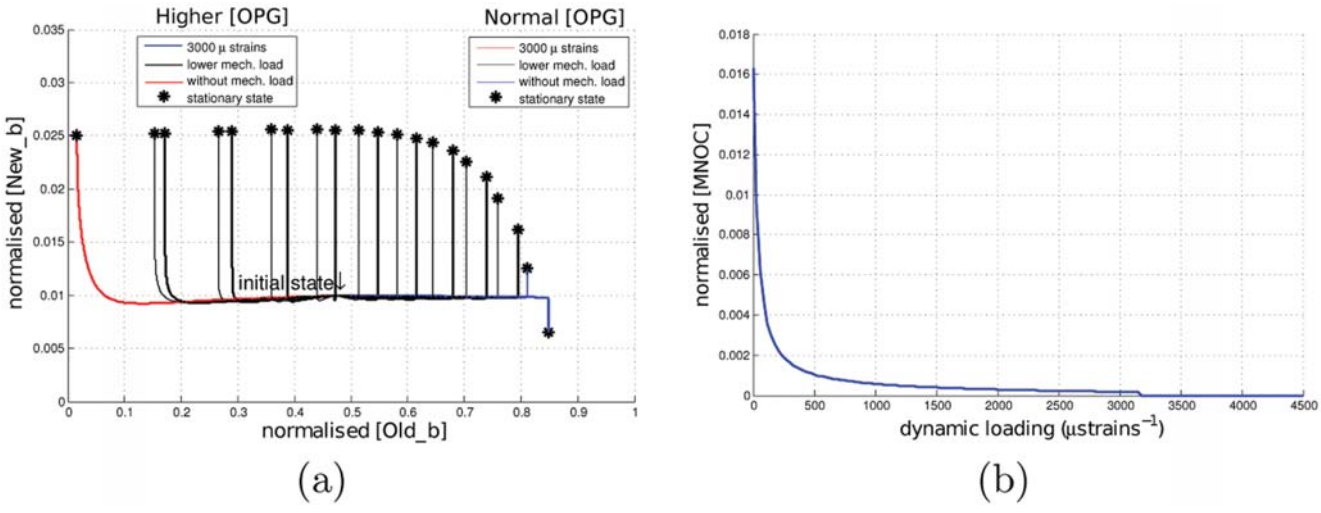

Figure 4. (a) A qualitative influence of OPG on bone density. β_1 decreases if the concentration/number of receptor-ligand bonds RANKL-RANK decreases. The rise of osteoprotegerin causes such a change. (b) Predicted dependence of osteoclast concentration (in stationary states) on dynamic loading.

the influence of various biochemical conditions under different mechanical stimuli. Figure 4 (a) shows the effects of decreasing of $[RR_0]$ (see relation (26) and reaction (1)) on the bone density. Such a decrease may be caused by higher levels of osteoprotegerin (OPG), which inhibits the receptor-ligand interaction. It is evident that a rise in OPG concentration will cause a growth of bone tissue or, more precisely, a decrease in the resorption, which leads to increased density of old bone tissue.

The formation of active multinucleated osteoclasts (1) (osteoclastogenesis) is also strongly influenced by mechanical stimuli, which can be seen from Figure 4 (b), where the stationary states of MNOC versus dynamic loading are plotted.

Discussion

The bone remodelling process and its controlling factors are not yet fully understood, especially at the cellular level, despite great advances in the last decade. It is critical to be able to predict the response of bone to varying conditions, both mechanical (e.g., after joint implants) and biological (e.g., after hormonal) changes. There are currently more than twenty models (not all of them are mentioned) that are used to simulate bone remodelling but are still not sufficient. However, they can be used for a better understanding of various concrete aspects related to bone remodelling, for example, endochondral ossification, role of microdamage in bone remodelling, pharmacological responses or histomorphometric indices. A vast majority of these models, except for the biochemical models[18,40,41], the mathematical model of Rattanakul[42], the reaction-diffusion models[43], and the optimisation model[44,45], are based solely on mechanical stimuli[46-53] and do not take into account dynamic stimuli. The model presented here combines both of these features. Moreover, the positivity of all concentrations is ensured for all physiological strains in human bone and the correct ratios of all the involved cell types (e.g. approx. 5% of *OB*) are predicted. The model parameters are realistic and measurable, at least in principle. There is exactly one positive stationary solution for the determined set of parameters which is asymptotically stable, and "exercise" (higher dynamic load) has positive effect on osteogenesis (bone formation exceeds resorption). Since the model describes the influence of dynamic loading on reaction rates, it allows for one to study the effects of the frequency of the applied loading on the bone remodelling process. Also, in the case of no mechanical stimuli (e.g., femur in cast), the bone density is not predicted to drop to zero. The model also distinguishes between bone being resorbed (Old_B) and bone tissue being formed (New_B) after a certain time. This distinction ensures that newly created bone tissue cannot be remodelled until it is fully developed (becoming New_B), which is consistent with the current understanding of bone remodelling.

The RANKL-RANK-OPG chain is frequently considered as one of the most important biochemical controls of the bone remodelling process, however there might be some other substantial mechanisms controlling the bone remodelling process[54]. Direct cellular contact between osteoclast precursors and stromal cells is needed for osteoclastogenesis[55]. This contact is mediated by receptors on osteoclasts, their precursor RANK, and the ligand RANKL on osteoblasts[56,57]. Osteoprotegerin (OPG) binds with higher affinity to RANK, which inhibits the receptor-ligand interaction, and reduces osteoclastogenesis[12]. Thus, the rise in OPG concentration results in a smaller number of resorbing osteoclasts (MNOC), which leads to higher bone tissue density. If it was accepted that a higher molar concentration of OPG led to a decrease in RANKL-RANK bonds, then the results shown on Figure 4 (a) would show the same qualitative behaviour. Moreover, Rubin discovered that dynamic loading down-regulates osteoclastic formation[3], which is also consistent with Figure 4 (b). This predicted

outcome can be considered as a form of validation.

Frost summarised his long-term observations from clinical praxis into a diagram showing the response of bone remodelling to mechanical stimuli[10]. He distinguished between compression and extension and expected a different bone response. Currently, it is known that *dynamic* loading is crucial for bone remodelling rather than static loading[2,9,12]. If this fact is accepted, then there cannot be any considerable difference between extension and compression since in everyday activities, such as walking and running, one process follows the other, and Figure 2 shows the same response that Frost observed.

In the presented model, there is no explicit dependence on several factors that strongly influence resorption, such as PTH, vitamin D, prostaglandins, and interleukins but it may be added, see below. However, these factors all signal the osteoblast cells, which appear to translate each signal into an appropriate RANKL or OPG output to control osteoclast development and, thus, resorption[12]. There is also a limitation in the application of our model to the scale of the desired results. Since the presented model is a concentration model, it cannot be used arbitrarily. The limitation is, of course, in the spatial precision of results. The minimal volume unit (finite element, or FE) should be sufficiently large to contain enough of all the substances entering the reaction schemes (1)-(5), namely MNOCs and *OB*s. It surely cannot be used on the length scales of BMU where it is no longer guaranteed that any MNOC is present. There are approximately 10^7 BMU in a human skeleton present at any moment (see section 3) and, because bones have a total volume of 1.75*l*, there is BMU per 0.175 mm^3 on average at any moment. In other words, the presented model cannot be used for length scales smaller than $\sqrt[3]{0.175\ mm^3}$ and we recommend that it is not used at length scales below $\sqrt[3]{0.5\ mm^3} \cong 0.8\ mm$.

The presented model can be implemented in any FEM model of bone (the parameters were set for human femur) and thus be used for predictions of distribution of bone density. The response of bone remodelling to changing environment, both mechanical (including effects of frequency) and biochemical, can be simulated and possible treatments can be proposed[58]. These simulations can be obtained when in each finite element the differential equations (9)-(13) are solved with site specific dynamic strains as input parameters (we assume a premixed, ideally stirred mixture of substances; further, the processes are considered to be isothermal at body temperature). These dynamic strains can be computed from balance of forces and momentum acting on bone (for example, muscle forces and forces acting on femur head can be used from[59]). Our ongoing applications of the model include simulations of the 3D geometries of the femur and vertebrae (FEM models).The preliminary results are encouraging and show the correct density distribution for the human femur compared to frontal plane slices of the human femur in anatomical atlases or for example[46]. Moreover, the effects of RANKL, OPG, PTH, estradiol, and NO on bone remodelling have been added to the presented model[58]. Because these effects are translated into an appropriate RANKL or OPG parameters, the number of bonds, *RR*, manages their impact. It enables a more precise formulation of the bone remodelling model and increases the applicability of the model to bone related diseases as can be seen in[58]. Moreover, it also considers microcracks which were found important in bone remodelling process[60]. Kurata et al. showed that higher microcrack density leads to higher RANKL levels at the site[61] which is now included in the model.

Acknowledgements

This research has been supported by the Czech Science Foundation project no. 106/08/0557 and no. 201/06/0352, by Research Plan No. AV0Z20760514 of the Institute of Thermomechanics AS CR, and by Research Plan MSM 6840770010 'Applied Mathematics in Technical and Physical Sciences' of the Ministry of Education, Youth and Sports of the Czech Republic.

Appendix A - List of parameters

$$\delta_1 = 4,\ \delta_3 = 2,\ \delta_4 = \frac{1}{7} = \delta_5,$$
$$\beta_1 = 0.6,\ \beta_3 = \frac{1}{2000},\ \beta_6 = 1.05,\ \beta_8 = \frac{1}{10},\ \beta_{11} = 1,\ \beta_{14} = \frac{1}{20}$$
$$J_{Old\_B} = J_{New\_B} = 2.610^{-4},\ J_3 = \frac{4}{25} J_5,$$
$$l_{1v} = -1.22\ 10^{-14}\ \frac{mol}{l},\ l_{2v} = 3.09\ 10^{-19}\ \frac{mol}{l},$$
$$l_{3v} = -3.49\ 10^{-17}\ \frac{mol}{l},\ l_{4v} = -1.39\ 10^{-17}\ \frac{mol}{l},$$
$$l_{5v} = 5.44\ 10^{-19}\ \frac{mol}{l}. \qquad \textbf{(A.1)}$$

Appendix B - Stationary solution and its stability

To have a concept of solution behaviour, it is useful to examine the existence and stability of stationary solutions. If the rate of forward reaction is assumed to be much greater than the backward rate ($k_{+\alpha} >> k_{-\alpha}, \forall\alpha \Leftrightarrow$ the forward reactions predominate over the backward ones), it will be possible to find a fixed point. Moreover, if we realize that all normalised concentration (n_i) should be positive (therefore stationary solutions are too) then there is exactly one positive stationary solution of the system (9)-(13):

$$\overline{n_{MCELL}} = 1/2\left(-\beta_1 + \sqrt{-\beta_1^2 + 4\,\frac{-D_1+J_3+J_{14}}{\delta_1}}\right)$$
$$\overline{n_{Old\_B}} = 1/2\left(-(\beta_3 + \overline{n_{MCELL}}) + \sqrt{(\beta_3 + \overline{n_{MCELL}})^2 + 4\,(J_{14} - D_2)}\right)$$
$$Sum_1 = 1/2\left((\beta_8 + \beta_6 - \overline{n_{Old\_B}}) + \sqrt{(\beta_8 - (\beta_6 - \overline{n_{Old\_B}}))^2 + 4\,\frac{J_{14}-D_3}{\delta_3}}\right)$$
$$Sum_2 = 1/2\left((\beta_{11} + Sum_1) - \sqrt{(\beta_{11} - Sum_1)^2 + 4\,\frac{J_{14}-D_4}{\delta_4}}\right)$$
$$\overline{New\_B} = 1/2\left((\beta_{14} + Sum_2) - \sqrt{(\beta_{14} - Sum_1)^2 + 4\,\frac{J_{14}-D_5}{\delta_5}}\right)$$
$$\overline{n_{Osteoid}} = Sum_2 - New\_B$$
$$\overline{n_{OB}} = Sum_1 - Sum_2. \qquad \textbf{(B.1)}$$

where $\bar{n}_i$ are positive normalised concentrations in a stationary state for the parameter values from the list of parameters (A.1)).

The stability of this fixed point (with parameter values from (A.1)) is guaranteed by Poincare-Ljapunov theorem. Firstly, a substitution $x_i=n_i-\bar{n}_i$ transforms the system (9)-(13) into a new one $\dot{x}=\mathbf{A}x+\mathbf{B}(t)x+f(t,x)$ that has a fixed point equal to zero. If we carry out this substitution, we find out that $\mathbf{B}(t)$, i.e.

$$\dot{x}=\mathbf{A}x+f(t,x)$$

where $f(t,x)=f(x)$ (the original system was autonomous) and $f(t)$ is a polynomial of the second order which is continuous, Lipschitz in x, and $\lim_{x\to 0}\frac{f(t,x)}{|x|}=0$ since all the linear terms are included in $\mathbf{A}x$. Finally, for parameter values from the list of parameters (A.1) the matrix $\mathbf{A}$ has all its eigenvalues real and negative. Thus, all the assumptions of Poincare-Ljapunov theorem are fulfilled and the stationary solution (B.1) is an asymptotically stable fixed point.

References

1. Li YJ, et al. Oscillatory fluid flow affects human marrow stromal cell proliferation and differentiation. J Orthop Res 2004;22:1283-9.
2. Ehrlich PJ, Lanyon LE. Mechanical strain and bone cell function: A review. Osteoporosis Int 2002;13:688-700.
3. Rubin J, Murphy T, Nanes MS, Fan X. Mechanical strain inhibits expression of osteoclast differentiation factor by murine stromal cells. Am J Physiol - Cell Physiol 2000; 278:C1126-32.
4. Rubin J, Murphy T, Zhu L, Roy E, Nanes MS, Fan X. Mechanical strain differentially regulates endothelial nitric-oxide synthase and receptor activator of nuclear kappa b ligand expression via erk1/2 mapk. J Biol Chem 2004; 278:34018-25.
5. Rubin J, Rubin C, Jacobs CR. Molecular pathways mediating mechanical signaling in bone. Gene 2006;367:1-16.
6. Valle F, Sandal M, Samori B. The interplay between chemistry and mechanics in the transduction of a mechanical signal into a biochemical function. Phys Life Rev 2007;4:157-88.
7. Lee WC, Maul TM, Vorp DA, Rubin JP, Marra KG. Effects of uniaxial cyclic strain on adipose-derived stem cell morphology, proliferation, and differentiation. Biomechan Model Mechanobiol 2007;6:265-73.
8. Adachi T, Sato K, Tomita Y. Directional dependence of osteoblastic calcium response to mechanical stimuli. Biomechan Model Mechanobiol 2003;2:73-82.
9. Heřt J, Přibylová E, Lišková M. Reaction of bone to mechanical stimuli. part 3: Microstructure of compact bone of rabbit tibia after intermittent loading. Acta Anat 1972; 82:218-30.
10. Frost HM. The Utah paradigm of skeletal physiology, volume second. Greece: ISMNI; 2004.
11. Frost HM. The utah paradigm of skeletal physiology: an overview of its insights for bone, cartilage and collagenous tissue organs. J Bone Miner Metab 2000;18:305-16.
12. Robling AG, Castillo AB, Turner CH. Biomechanical and molecular regulation of bone remodeling. Annu Rev Biomed Eng 2006;8:455-98.
13. Klika V and Maršík F. Coupling effect between mechanical loading and chemical reactions. J Phys Chem B 2009; 113:14689-97.
14. Lindsay R. What have we learned from clinical studies? fractures and the interactions of bone mass and remodeling. Osteoporosis Int 2003;14:S8-S11.
15. Bougherara H, Klika V, Maršík F, Mařík I, Yahia LH. A Novel Approach for Bone Remodeling After Prosthetic Implantation. In: Damage and Fracture Mechanics. Netherlands: Springer; 2009. p. 553-65.
16. Bougherara H, Klika V, Maršík F, Mařík I, Yahia LH. A new predictive model for monitoring bone remodeling. J Biomed Mater Res: A 2009; in press.
17. Maršík F, Klika V, Chlup H. Remodelling of living bone induced by dynamic loading and drug delivery - numerical modelling and clinical treatment. Math Comput Simul 2010;80:1278-88.
18. Lemaire V, Tobin FL, Greller LD, Cho CR, Suva LJ. Modeling the interactions between osteoblast and osteoclast activities in bone remodeling. J Theor Biol 2004; 229:293-309.
19. Keener J and Sneyd J. Mathematical Physiology, I: Cellular Physiology. New York: Springer Science+Business Media; 2009.
20. Nicolis G and Prigogine I. Selforganization in nonequilibrium systems. New York: Wiley; 1977.
21. Boyle WJ, Simonet WS, Lacey DL. Osteoclast differentiation and activation. Nature 2003;423(3):337-42.
22. Hill PA. Bone remodelling. Br J Orthod 1998;25:101-7.
23. Mundy GR, Boyce B, Hughes D, Wright K, Bonewald L, Dallas S. The effects of cytokines and growth factors on osteoblastic cells. Bone 1995;17:71S-75S.
24. Pfeilschifter J, Seyedin SM, Mundy GR. Transforming growth factor beta inhibits bone resorption in fetal rat long bone cultures. J Clin Invest 1988;82:680-5.
25. Vaira S, Alhawagri M, Anwisye I, Kitaura H, Faccio R, Novack DV. Rela/p65 promotes osteoclast differentiation by blocking a RANKL-induced apoptotic JNK pathway in mice. J Clin Invest 2008;118:2088-97.
26. Ruffoni D, Fratzl P, Roschger P, Klaushofer K, Weinkamer R. The bone mineralization density distribution as a fingerprint of the mineralization process. Bone 2007;40:1308-19.
27. Kanehisa J and Heersche JN. Osteoclastic bone resorption: in vitro analysis of the rate of resorption and migration of individual osteoclasts. Bone 1988;9:73-9.
28. Frost HM. Tetracycline-base histological analysis of bone remodelling. Calcif Tissue Res 1969;(3):211-37.
29. Parfitt AM. Osteonal and hemi-osteonal remodeling: the spatial and temporal framework for signal traffic in adult human bone. J Cell Biochem 1994;55:273-86.
30. Rucker D, Hanley DA, Zernicke RF. Response of bone to exercise and aging. Locomot Syst 2002;9(1-2):6-22.
31. Eriksen EF and Kassem M. The cellular basis of bone re-

modelling. Triangle 1992;31:45-57.
32. Manolagas SC. Editorial:cell number versus cell vigor-what really matters to a regenerating skeleton? Endocrinology 1999;140:4377-81.
33. Jee WS. The skeletal tissues. In: Weiss, L (ed) Histology: cell and tissue biology 5th ed. 1983
34. Sugawara Y, Kamioka H, Honjo T, Tezuka K, Takano-Yamamoto T. Three-dimensional reconstruction of chick calvarial osteocytes and their cell processes using confocal microscopy. Bone 2005;36:877-83.
35. Rho JY, Ashman RB, Turner CH. Young's modulus of trabecular and cortical bone material: ultrasonic and microtensile measurements. J Biomech 1993;26:111-9.
36. Weinstein RS et al. Promotion of osteoclast survival and antagonism of bisphosphonate-induced osteoclast apoptosis by glucocorticoids. J Clin Invest 2002;109:1041-8.
37. Helgason B, Perilli E, Schileo E, Taddei F. Mathematical relationships between bone density and mechanical properties: A literature review. Clin Biomech 2008;23:135-46.
38. Hedgecock NL, et al. Quantitative regional associations between remodeling, modeling, and osteocyte apoptosis and density in rabbit tibial midshafts. Bone 2007;40:627-37.
39. Hodgskinson R and Currey JD. Young's modulus, density and material properties in cancellous bone over a large density range. J Mater Sci Mater Med 1992;3:377-81.
40. Komarova SV, Smith RJ, Dixon SJ, Sims SM, Wahlb LM. Mathematical model predicts a critical role for osteoclast autocrine regulation in the control of bone remodeling. Bone 2003;33:206-15.
41. Müller R. Long-term prediction of three-dimensional bone architecture in simulations of pre-, peri- and postmenopausal microstructural bone remodeling. Osteoporosis Int 2005;16:S25-S35.
42. Rattanakul C, Lenbury Y, Krishnamara N, Wollkind DJ. Modeling of bone formation and resorption mediated by parathyroid hormone: response to estrogen/pth therapy. Biosystems 2003;70:55-72.
43. Matsuura Y, Oharu S, Takata T, Tamura A. Mathematical approaches to bone reformation phenomena and numerical simulations. J Comput Appl Math 2003;158:107-19.
44. Fernandes PR, Folgado J, Jacobs C, Pellegrini V. A contact model with ingrowth control for bone remodelling around cementless stems. J Biomech 2002;35:167-76.
45. Chen G, Pettet GJ, Pearcy M, McElwain DS. Modelling external bone adaptation using evolutionary structural optimisation. Biomechan Model Mechanobiol 2007;6:275-85.
46. Carter DR. Mechanical loading history and skeletal biology. J Biomech 1987;20:1095-109.
47. Huiskes R et al. Adaptive bone-remodeling theory applied to prosthetic-design analysis. J Biomech 1987;20:1135-50.
48. Beaupre GS, Orr TE, Carter DR. An approach for time-dependent bone modeling and remodeling-application: a preliminary remodeling simulation. J Orthop Res 1990; 8:662-70.
49. Doblaré M, García JM. Anisotropic bone remodelling model based on a continuum damage-repair theory. J Biomech 2002;35:1-17.
50. Ruimerman R, Hilbers PA, van Rietbergen B, Huiskes R. A theoretical framework for strain-related trabecular bone maintenance and adaptation. J Biomech 2005;38:931-41.
51. Turner CH, Anne V, Pidaparti RV. A uniform strain criterion for trabecular bone adaptation: Do continuum-level strain gradients drive adaptation? J Biomech 1997; 30:555-63.
52. García-Aznar JM, Rueberg T, Doblaré M. A bone remodelling model coupling microdamage growth and repair by 3d bmu-activity. Biomechan Model Mechanobiol 2005; 4:147-67.
53. Martínez-Reina J, García-Aznar JM, Dominguez J, Doblaré M. A bone remodelling model including the directional activity of bmus. Biomechan Model Mechanobiol 2009;8:111-27.
54. Pogoda P, Priemel M, Ruegger JM, Amling M. Bone remodeling: new aspects of a key process that controls skeletal maintenance and repair. Osteoporosis Int 2005; 16:S18-S24.
55. Takahashi N, et al. Induction of calcitonin receptors by 1 alpha, 25-dihydroxyvitamin d3 in osteoclast-like multinucleated cells formed from mouse bone marrow cells. Endocrinology 1988;123:1504-10.
56. Simonet WS, et al. Osteoprotegerin: A novel secreted protein involved in the regulation of bone density. Cell 1997; 89:309-19.
57. Tsuda E et al. Isolation of a novel cytokine from human fibroblasts that specifically inhibits osteoclastogenesis. Biochem Biophys Res Commun 1997;234:137-42.
58. Klika V, Maršík F, Mařík I. Influencing the Effect of Treatment of Disease Related to Bone Remodelling by Dynamic Loading. In: Dynamic Modelling. Vienna: INTECH. February 2010.
59. Bergmann G, Graichen F, Rohlmann A. Hip joint loading during walking and running, measured in two patients. J Biomech 1993;26:969-90.
60] Da Costa Gomez TM, et al. Up-regulation of site-specific remodeling without accumulation of microcracking and loss of osteocytes. Bone 2005;37:16-24.
61. Kurata K, Heino TJ, Higaki H, Vaananen HK. Bone marrow cell differentiation induced by mechanically damaged osteocytes in 3d gel-embedded culture. J Bone Min Res 2006;21:616-25.